

## Dynamics of Laser-Plasma Interaction at $10^{18}$ W/cm<sup>2</sup>

M. P. Kalashnikov, P. V. Nickles, Th. Schlegel, M. Schnuerer, F. Billhardt, I. Will, and W. Sandner\*

*Max-Born-Institut, Rudower Chaussee 6, 12489 Berlin, Germany*

N. N. Demchenko

*P. N. Lebedev Physical Institute, Leninsky prospect 53, 117924 Moscow, Russia*

(Received 24 November 1993)

The interaction of 2 ps FWHM laser pulses with solid targets at intensities  $10^{16}$ – $10^{18}$  W/cm<sup>2</sup> is studied for two essentially different cases of laser front steepness resulting in preplasma and preplasma-free interaction. Red and blue frequency shifts of a backscattered fundamental wave and its second harmonic depending on the incident laser pulse shape are observed. They are associated with Doppler shifts corresponding to inward or outward movement of the critical density surface. A model including ponderomotive force was developed to explain the experimental results.

PACS numbers: 52.35.Mw, 52.40.Nk, 52.50.Jm, 52.65.+z

The major progress in compact solid state laser sources has allowed recent experiments [1–3] to be carried out in which the plasma is created by laser radiation with extremely high intensity, in the range of  $10^{18}$  W/cm<sup>2</sup>. Under those conditions, the process of interaction is characterized by relativistic electron oscillations in the intense electromagnetic field of the laser light wave. Plasmas produced at such intensities are expected to show significant influence of strong ponderomotive forces [4,5]. For instance, strong spatial density modulations and “hole boring” effects have been predicted by theory [6]. Despite a relatively large amount of laser-plasma interaction investigations at the level of incident laser flux density  $< 10^{18}$  W/cm<sup>2</sup>, the influence of ponderomotive pressure and relativistic effects as well as incident pulse shape on plasma dynamics is not fully understood. Because of a rather low plasma ignition threshold ( $10^9$ – $10^{11}$  W/cm<sup>2</sup>) the pulse background to peak contrast ratio and the steepness of the rising laser pulse front determine parameters of the preplasma from which the high-intensity interaction starts.

In this Letter we report on spectral modifications in the backscattered fundamental wave and its second harmonic observed experimentally, as well as on results of corresponding computer simulations. It is shown for the first time that, at a level of incident intensities  $10^{16}$ – $10^{18}$  W/cm<sup>2</sup>, the critical density surface moves either towards the overdense plasma region or in the opposite direction depending on the steepness of the pulse front.

The experiments were carried out with a CPA laser delivering output pulses of 1.5–2 ps duration at an energy level of 1 J [7]. The beam was focused by a  $f/2$  aspherical lens on Al-coated ( $1 \mu\text{m}$ ) optical flat glass targets. Under the best focusing conditions 40% of the incident energy has been measured in a spot of  $4 \mu\text{m}$  in diameter, resulting in flux densities up to  $2 \times 10^{18}$  W/cm<sup>2</sup>. The high ASE contrast ( $> 4 \times 10^9$ ) [7] was achieved mainly through the fiberless CPA laser design.

An improvement of the contrast to  $10^{10}$  and a steepening of the rising pulse front was realized with a nonlinear absorber cell placed after the grating compressor. This case is referred to as “clean” pulse.

Spectral distributions of the backscattered fundamental wave and the second harmonic have been investigated for these two cases of pulse shapes (Fig. 1). The measurement of a spectral shift in backscattered radiation resulting from plasma movement is a powerful tool of plasma dynamics investigations in the vicinity of critical density [8]. That is especially the case for a short pulse laser-plasma interaction when the density profile is rather narrow and has a steep gradient, in contrast to experiments carried out with rather long laser pulses [9]. Characteristic features of the backscattered radiation are depicted in Figs. 2(a) and 2(b). First, we have found that, depending on the level of the incident flux and steepening of the laser pulse front, the backscattered spectra are broadened, modulated, and shifted either to the blue or to the red. Second, the fundamental wave and its second harmonic have similar wavelength shifts  $\Delta\lambda/\lambda$ . In all experiments

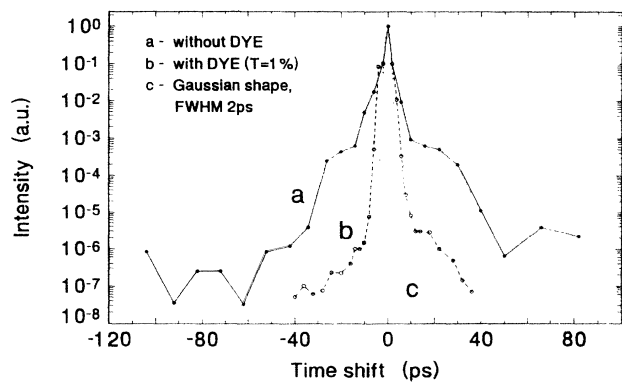


FIG. 1. Third order correlation traces of compressed laser pulses with FWHM 2 ps. Curve *a*: without dye absorber; curve *b*: steepened by the dye; curve *c*: Gaussian shaped pulse.

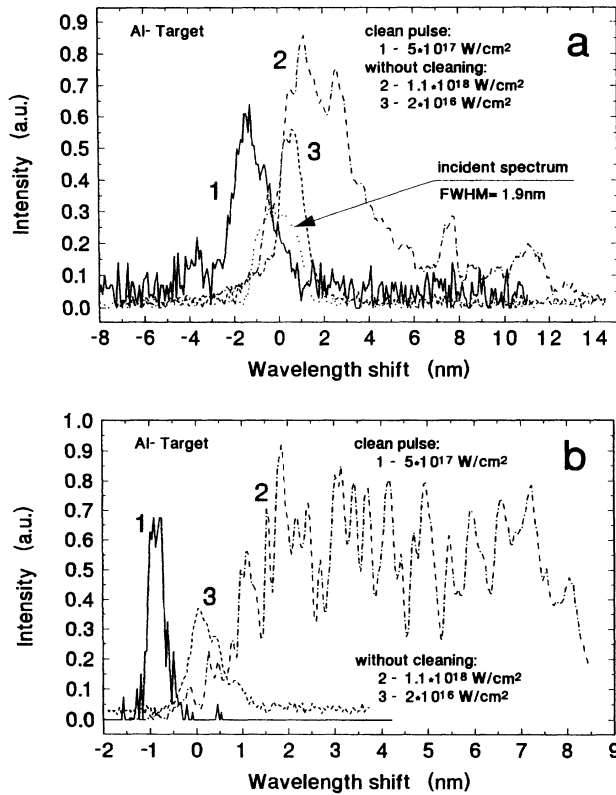


FIG. 2. Typical spectral distributions of the backscattered fundamental wave (a) and second harmonic (b) for different pump pulses.

with a nonsteepened pulse the backscattered spectrum is broadened and redshifted. This corresponds to [1], but in our case of much higher peak intensities we get a rather strong effect of the ponderomotive force on plasma dynamics. The spectra show modulations which are more noticeable for the second harmonic. However, in the case of clean pulse both spectra are less strongly modulated and a slight blueshift  $\sim 1-3$  nm is observed. Red and blue components are visible in intermediate cases when the rising pulse front is less steepened due to nonoptimum dye concentration.

Assuming that for the nonsteepened pulse the redshift in the backscattered spectra is determined by the Doppler shift which results from the inward movement of plasma under the influence of the ponderomotive force we have estimated the velocity of critical density movement (Fig. 3). Maximum values  $dR_c/dt \approx 2.5 \times 10^8$  cm/s ( $R_c$  denotes the distance of the critical density layer to the initial target surface) are deduced for angles close to  $40^\circ$ . In addition, the result of a simple estimate [6]—balance between the momentum flux of mass flow and the light pressure—is plotted (curve 4). It differs from the experimental results for laser intensities  $\leq 10^{17}$  W/cm<sup>2</sup>, when the thermal pressure cannot be neglected further in com-

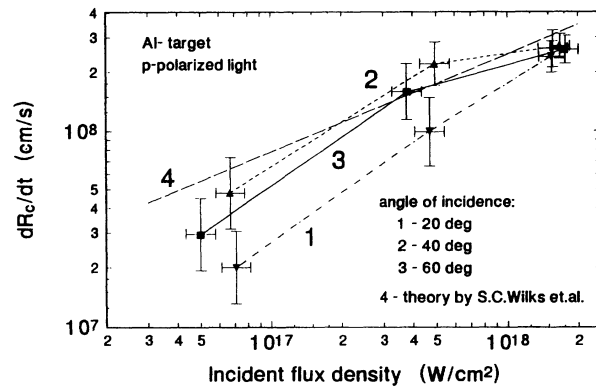


FIG. 3. Dependence of critical density velocity  $dR_c/dt$  evaluated from the redshift of the second harmonic spectra on the incident flux density at different angles of incidence. Pulse shape corresponds to curve a in Fig. 1.

parison with the ponderomotive one. Besides that this simple estimate cannot explain the dependence of frequency shifts on the angle of incidence.

To understand the complicated behavior of the short-pulsed generated plasma flow caused by the competition of thermal and ponderomotive forces, we have developed a theoretical model which includes one-dimensional hydrodynamics in plane geometry together with Maxwell equations for the electromagnetic field of the laser light wave. The model considers the influence of the ponderomotive forces self-consistently. In comparison to previous investigations [10], oblique incidence of the electromagnetic waves with  $s$  and  $p$  polarization was assumed.

In the relativistic case the plasma frequency becomes  $\omega_p = 4\pi e^2 n_e / m_0 \gamma_0$ ,

$$\gamma_0 = \left[ 1 + \frac{1}{2} \left( \frac{e|E|}{\omega m_0 c} \right)^2 \right]^{1/2},$$

where  $\omega$  is the laser frequency. Now the critical plasma density (determined from  $\omega_p = \omega$ ) depends on the value of the electric field. Another important effect taken into account is the generation of hot electrons in the resonant electromagnetic field of a  $p$  polarized light wave. The consideration of laser energy dissipation due to this process [11] allows the correct description of the resonant field. In the discussed circumstances hot electron generation is the dominant process which limits this field. A simple estimate assuming a linear density profile with the characteristic length of inhomogeneity  $L_c = [(1/\rho)d\rho/dz]^{-1}$  gives for the hot electron collisional frequency

$$\frac{\nu_h}{\omega} + \frac{\nu_{ei}}{\omega} = \frac{e\alpha_0 |H_c|}{\omega m_0 c} \left[ \left( 1 + \frac{\pi e\alpha_0 |H_c| L_c}{2m_0 c^2} \right)^2 - 1 \right]^{-1/2},$$

where  $\nu_{ei}$  characterizes Coulomb scattering of electrons by ions,  $\alpha_0 = \sin\theta_0$ ,  $\theta_0$  is the angle of incidence, and  $H_c$

is the magnetic field in the resonance region. The relation becomes incorrect for very large ponderomotive forces, when the density gradients strongly increase ( $L_c \rightarrow 0$ ). In this limit, we used a value  $\nu_h/\omega = 1/4$  deduced from Brunel's capacitor model [12]. Density profiles for both cases of pulse shapes (Fig. 1),  $p$ -polarized light, and an angle of incidence  $40^\circ$  are presented on Figs. 4(a) and 4(b).

The plasma accumulates in the overcritical region for as long as ponderomotive forces exceed thermal pressure [see Figs. 4(a) and 4(b)]. The critical density located in this region we call the "main" critical. In addition, narrow overcritical peaks appear in the undercritical plasma. Our computer simulations have shown that the strength of the peaks, direction, and velocity of their movement depend on the shape of the laser pulse front and the angle of incidence. In both cases of laser pulse shape the characteristic length of inhomogeneity becomes too small in the turbulent plasma range at high laser intensities to give rise to significant scattering processes [13]. The numerical data show, after an intermediate reduction of the absorption on the leading edge of the laser pulses, a subsequent increase of the time-integrated

relative absorption for main pulse intensities rising up to maximum values greater than  $10^{17}$  W/cm<sup>2</sup>.

For the high steepened pulse front [Fig. 4(b)] because of the small scale length of the plasma, a very small distance of shock wave movement is needed to produce a thermal pressure which can overcome the ponderomotive one. Because of the small width of the overcritical peaks ( $<0.05\lambda_0$ ), the incident laser wave propagates through these peaks and irradiates the main critical surface. In this case, the pressure at the front of the evaporation wave is much higher than the light pressure in the vicinity of the critical density. As a result the critical density front moves in the direction of the plasma corona producing a blue frequency shift in the scattered radiation. That is in agreement with our experimental results.

For an "extended" density profile [Fig. 4(a)], plasma movement in the region of critical density has a strong dependence on the angle of incidence. For an angle of  $20^\circ$  we have found short-lived narrow overcritical peaks in the undercritical plasma. The peaks appear and disappear in an irregular way similar to the situation described in [14]. Usually, there are several overcritical maxima in the undercritical density region and each of them has two critical surfaces and two corresponding field resonances. Under the influence of the ponderomotive forces in these resonances, the lifetime of the peaks is limited. The laser radiation is partly absorbed and scattered by them and consequently the flux density incident on the permanently existing main critical surface is modulated. Similar to the experimental observations, the main critical density region exhibits an inward movement with a velocity of  $dR_c/dt = 4.7 \times 10^7$  cm s<sup>-1</sup>.

For the angle of incidence  $40^\circ$  corresponding to the angle of maximum resonance absorption, we found a rather broad overcritical density peak arising in the underdense plasma region [see Fig. 4(a)]. In this case, the resonant field is located only on the irradiated side of the density peak. The main critical surface is fully screened by this peak. Later on, this shock wave moves inwards [see Fig. 4(a)] under the influence of the ponderomotive pressure. The velocity of this inward movement  $dR_c/dt = 2.7 \times 10^8$  cm s<sup>-1</sup> is in good agreement with experimental values deduced from wavelength shifts of backscattered spectra (Fig. 3). During the action of the main laser pulse, the process of formation and movement of such strong overcritical peaks repeats several times. In Fig. 5, the movement of the outmost lying critical surface as a function of time is plotted. The dominating action of either plasma or radiation pressure on the density maxima (some of them are marked with arrows) in dependence on the laser pulse shape is clearly shown.

For the angle of incidence  $60^\circ$  only one shock wave arises under the action of the ponderomotive pressure at the main critical surface. Because there is no more screening of the light wave due to additional density peaks, the speed of the main critical surface movement

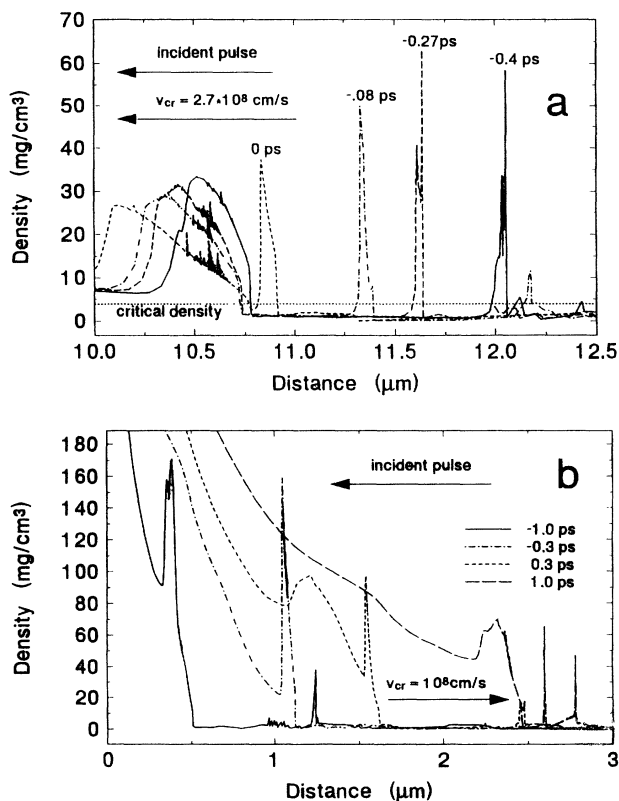


FIG. 4. Density profiles in the vicinity of the critical surface at different times related to the pulse maximum ( $I_L = 5 \times 10^{17}$  W/cm<sup>2</sup>). An angle of incidence  $40^\circ$  was assumed. (a) and (b) correspond to pulse shape curves  $a$  and  $b$  in Fig. 1, respectively.

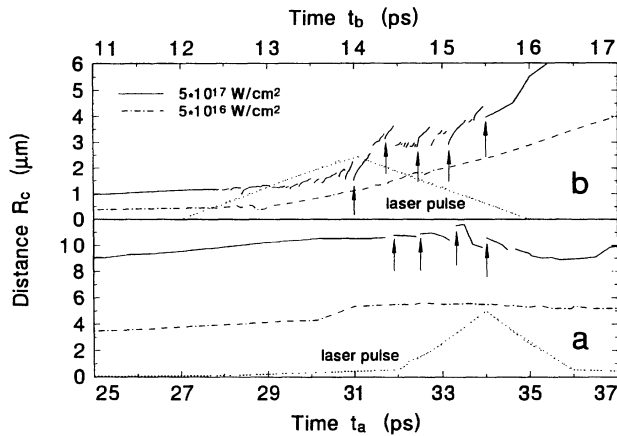


FIG. 5. Position of the outmost overcritical density peak as a function of time for two laser intensities. (a) and (b) correspond to pulse shape curves *a* and *b* in Fig. 1, respectively. Arrows mark some of the newly appearing overcritical density peaks.

( $dR_c/dt = 10^8 \text{ cm s}^{-1}$ ) exceeds the corresponding velocity for smaller angles of incidence. It is smaller than the speed of the overcritical peak movement at the angle of incidence optimum for resonance absorption because of the larger thermal pressure at critical density.

In conclusion, we have found that for extremely high-intensity laser pulses plasma dynamics in the vicinity of the critical density may change essentially depending on the steepness of the incident laser pulse. At the relatively high level of the prepulse, the critical density surface may be driven by the ponderomotive force in the overdense region with a very high velocity ( $dR_c/dt \approx 3 \times 10^8 \text{ cm s}^{-1}$  for a flux density  $\sim 10^{18} \text{ W/cm}^2$ ). Redshifts in the backscattered radiation and strong modulations of the second harmonic spectrum are observed. Both theory and experiment show the same dependence of red frequency shifts on angles of laser incidence. The maximum of the redshift we find at angles of  $\theta \approx 40^\circ$  which is also the optimum for resonance absorption.

For our experimental conditions we assume that resonance absorption and anharmonic oscillations of electrons in an intense electromagnetic wave [15] are responsible for the second harmonic generation. It is known that, for effective harmonic generation, matching conditions have to be fulfilled [16, 17]. In the case of a rapidly modifying density profile, one can suppose that conditions for optimum harmonic generation are fulfilled in short time intervals resulting in fast temporal and hence spectral modulations of the emitted radiation.

In contrast, when the laser pulse is clean and the plasma gradient is steep, the critical density moves only in the direction of plasma corona, leading to blueshifts in the backscattered radiation. This complicated plasma behavior should be taken into account in the interpretation of spectroscopic data obtained in short-pulse laser-matter interaction experiments.

This research was partly supported by the Bundesministerium für Forschung und Technologie (Project No. 211-5291-LAS, 1991) and Senatsverwaltung Berlin für Wissenschaft und Forschung.

\*Also with the Department of Physics, University of Tennessee, Knoxville, TN 37996-1200.

- [1] G. Mourou and D. Umstadter, *Phys. Fluids B* **4**, 2315 (1992); X. Liu and D. Umstadter, *Phys. Rev. Lett.* **69**, 1935 (1992).
- [2] F. G. Patterson, R. Gonzales, and M. D. Perry, *Opt. Lett.* **16**, 1107 (1991).
- [3] J. K. Kmetec, C. L. Gordon III, J. J. Macklin, B. E. Lemoff, G. S. Brown, and S. E. Harris, *Phys. Rev. Lett.* **68**, 1527 (1992).
- [4] H. Hora, *Physics of Laser Driven Plasmas* (Wiley, New York, 1981).
- [5] P. Mulser, *J. Opt. Soc. Am. B* **2**, 1814 (1985).
- [6] S. C. Wilks, W. L. Kruer, M. Tabak, and A. B. Langdon, *Phys. Rev. Lett.* **69**, 1383 (1992).
- [7] F. Billhardt, M. Kalashnikov, P. V. Nickles, and I. Will, *Opt. Commun.* **98**, 99 (1993).
- [8] N. G. Basov, A. S. Rupasov, G. V. Sklizkov, A. S. Shikanov, Yu. A. Zakharenkov, and N. N. Zorev, *Heating and Compression of Laser Irradiated Targets* (Cambridge Univ. Press, Cambridge, 1986); W. B. Fechner, C. L. Shepard, Gar. E. Busch, R. J. Schroeder, and J. A. Tarvin, *Phys. Fluids* **27**, 1552 (1984).
- [9] R. A. Maddever, B. Luther-Davies, and R. Dragila, *Phys. Rev. A* **41**, 2154 (1990); **41**, 2165 (1990).
- [10] N. N. Demchenko, V. B. Rosanov, and M. N. Tagviashvily, *Fiz. Plazmy* **16**, 812 (1990) [*Sov. J. Plasma Phys.* **16**, 472 (1990)].
- [11] P. Gibbon and A. R. Bell, *Phys. Rev. Lett.* **68**, 1535 (1992).
- [12] F. Brunel, *Phys. Rev. Lett.* **59**, 52 (1987).
- [13] W. L. Kruer, *The Physics of Laser Plasma Interactions* (Addison-Wesley, New York, 1988).
- [14] N. E. Andreev, V. P. Silin, and G. L. Stenchikov, *Sov. Phys. JETP* **51**, 703 (1980).
- [15] L. D. Landau and E. M. Lifshitz, *The Classical Theory of Fields* (Pergamon Press, New York, 1975).
- [16] G. Auer, K. Sauer, and K. Baumgärtel, *Phys. Rev. Lett.* **42**, 1744 (1979).
- [17] R. Dragila, *J. Appl. Phys.* **53**, 865 (1982).